February 18, 2000

Radio Detection of a Rapid Disturbance Launched by a Solar Flare

S. M. White, P. Janardhan[1] and M. R. Kundu

Astronomy Department, University of Maryland, College Park, MD 20742

white,jerry,kundu@astro.umd.edu

ABSTRACT

We report the direct observation of motion associated with a solar flare at a speed of 26000 km s^{-1}. The motion is seen from a radio source at 0.33 GHz, which suddenly starts moving during the flare. At its peak the radio source covers a quiet region of dimension $500''$. Emission from any given location is sporadic. The disturbance itself does not seem to radiate, but it excites coronal features which continue to radiate after it passes. The inferred velocity is larger than any previously inferred velocity of a disturbance in the solar atmosphere apart from freely–streaming beams of accelerated electrons. The observed motion of the source at a fixed frequency, low polarization and moderate bandwidth are more consistent with the typical properties of moving Type IV radio bursts than with classical coronal–shock–associated Type II bursts, but any disturbance at such a high velocity must be highly supersonic and should drive a shock. We speculate that the disturbance is associated with the realignment of magnetic fields connecting different portions of an active region.

Subject headings: shock waves — Sun: atmospheric motions, flares, radio radiation, corona

1. INTRODUCTION

The study of moving disturbances in the solar atmosphere is an important topic for several reasons: such disturbances may lead to shocks in the solar wind which have terrestrial consequences, and because they may be studied in detail at relatively close range they

[1]on leave from the Physical Research Laboratory, Ahmedabad, India

may reveal physical processes which are important but difficult to study in more distant astrophysical settings. A number of such disturbances are recognized. Some of the earliest detections were inferred from radio observations: beams of accelerated electrons freely streaming at $\sim$ 40000 km s^{-1} which produce Type III radio bursts (Wild 1950a), coronal shocks at 500 – 2000 km s^{-1} which produce Type II radio bursts (Wild 1950b; Wild et al. 1954), and moving features at 200 – 1600 km s^{-1} which produce moving Type IV radio bursts (Weiss 1963). In the chromosphere "Moreton waves" are detected in Hα images of solar flares at velocities as high as 4000 km s^{-1} (Moreton 1961; Athay & Moreton 1961; Ramsey & Smith 1966). Erupting prominences with speeds of hundreds of km s^{-1} have been known for some time, and coronal mass ejections (CMEs) were detected when the first space–borne coronagraph operated on *SKYLAB* (MacQueen et al. 1974). More recently, the SXT telescope on the *Yohkoh* satellite has detected ejecta at soft X–ray–emitting temperatures with velocities of order 30 – 300 km s^{-1} (Shibata et al. 1992) and the EIT telescope on *SOHO* has detected flare–associated disturbances from the motion produced in coronal features as the disturbance passes by (Thompson et al. 1999): velocities are of order 100 – 250 km s^{-1}.

In this paper, we report radio observations of motion of a disturbance in the solar corona which reaches a speed as high as 26000 km s^{-1}, i.e., faster than any other known form of coronal disturbance apart from free–streaming electrons. The motion occurred in association with a GOES class C9 flare whose other properties have already been described extensively by Silva et al. (1996). In this paper we focus on imaging observations of the event made at 0.333 GHz with the Very Large Array radiotelescope[2].

2. THE OBSERVATIONS

The flare occurred at about S16W18 in AR 6944, starting at 20:21:30 UT (all times quoted in this paper will be in UT) on 1992 January 7. Both radio and X–ray data show two main peaks, occurring at around 20:22 and 20:25, respectively (Silva et al. 1996). The VLA was operated in frequency–switching mode for these observations. During the first peak from 20:21 to 20:24, the VLA was observing in the 5 GHz band: these observations were discussed by Silva et al. (1996). During the second peak from 20:24:21 to 20:27, the VLA observed at 0.33 and 1.4 GHz simultaneously, and we discuss these lower–frequency data here. The time resolution of the data is 3.3 s; the VLA was in "B" configuration and

---

[2]The VLA is operated by the National Radio Astronomy Observatory, which is a facility of the National Science Foundation operated under cooperative agreement by Associated Universities, Inc.

the 0.33 GHz images shown are restored with a 40″ circular beam. The effective resolution is probably somewhat larger than this due to coronal scattering (Bastian 1994). Radio images at 9 selected times are shown in Figure 1, overlaid on a Kitt Peak magnetogram of the region. The flare occurred in a complex consisting of two adjoining labelled regions occupying the bottom right corner of the images, AR 6993 to the north and AR 6994 to the south. AR 6994 was magnetically the more complex of the two regions (Silva et al. 1996).

Two continuum "noise storm" sources were present at 0.33 GHz throughout the day, and are labelled "NS" in the panels. These sources are commonly present over the leading spots of vigorous active regions, and produce continuum emission, typically from 0.1 to 0.4 GHz, which can vary on timescales as short as minutes (Kai et al. 1985). They are not associated with flares. On this day the western NS source was the stronger of the two and lay over the positive–polarity leading spot of AR 6993. This source was 100% left circularly polarized (LCP), as expected for plasma emission in the ordinary (o) mode from upgoing magnetic fields (Melrose 1985), with a brightness temperature T_B ranging from $0.5 - 2 \times 10^9$ K during the period discussed here (these numbers are actually lower limits since we suspect that the true sizes of the noise storm sources are smaller than their apparent sizes; T_B is derived from flux per beam following standard formulae). The eastern noise storm source lies over the negatively polarized leading spot of AR 6996, and is 100% right circularly polarized (RCP). Its brightness temperature is an order of magnitude weaker (range $0.5 - 2 \times 10^8$ K), but both have brightness temperatures too high to be explained by simple thermal emission, consistent with the accepted interpretation that the emission mechanism is coherent plasma emission (Kai et al. 1985). Note that the contour levels in Fig. 1 differ in different regions of the image for clarity of presentation (see caption).

The optical, X–ray and higher–frequency radio emission in this flare all arose in the region of mixed polarity closest to the bottom right corner of the panels in Fig. 1 (marked by a plus symbol in the first panel of Fig. 1). When observations at 0.33 GHz commenced at 20:24:21, emission close to this location may be seen as the source elongated from south–east to north–west at 20:24:31. The contours shown are the LCP contours. The initial flare source is clearly elongated by comparison with the noise storm sources. The flare source is observed to be stationary from 20:24:21 to 20:24:31, and then appears to move rapidly to the north–east, in the direction of apparent disk center (the top three frames of Fig. 1). The direction of motion is roughly orthogonal to the major axis of the source prior to the motion. Note that the noise storm sources are stationary throughout. Prior to the onset of motion at 20:24:31, the peak T_B in the flare source in LCP is 6×10^8 K, and it is 40% – 50% polarized in the LCP sense.

Following the initial motion the radio flux actually drops (e.g., 20:24:51) and is close to but not coincident with the initial flare source. In subsequent frames brightening is seen progressively further to the north–east, reaching as far as the noise storm source in AR 6996 but no further. The images do not show continuous motion of a single discrete source, but rather the successive brightening of different regions between the two noise storms. The different features fluctuate rapidly in brightness, so that the location of the brightest emission switches quickly between locations near the original flare source, just south of disk center and near the north–east noise storm (these three locations are all bright at 20:25:04). By 20:25:27, near peak flux levels, the brightest emission is actually closer to the north–eastern noise storm than it is to the original flare source. Peak brightness temperatures in the extended flare source range from $2-4 \times 10^8$ K. At its peak at 20:25:20, the total flux from the flare source is of order 150 sfu, while the brighter noise storm is about 50 sfu in LCP only. The polarization of the brighter sources is generally small ($\leq 20\%$, i.e., much smaller than the polarization of the flare source prior to the motion) and is predominantly LCP to the south–west and RCP near the north–eastern noise storm, consistent with the polarizations of the noise storms in the two locations. No emission is seen to arise in any direction other than north–east of the original flare location. Both noise storm sources show fluctuations in intensity during the period when the moving source is present, but neither is obviously related to the motion of the flare source. The magnetogram indicates that there are no obvious photospheric features corresponding to the regions which appear bright in the bottom three frames of Fig. 1, and SXT images show no distinct coronal features in this region of the solar atmosphere.

At 1.4 GHz, three distinct sources are detected: one, probably representing thermal emission from post–flare loops, at the site of the original flare (the plus symbol in the top left panel of Fig. 1); a second over the trailing sunspot in AR 6993; and a third just south of the trailing spot in AR 6994. The positions of the latter two sources are denoted by white plus symbols in the bottom left panel of Fig. 1. The time profiles of the latter two sources are similar to each other and to that of the P band emission. Both are highly RCP polarized (consistent with *o* mode emission from the downgoing magnetic fields at their locations) and have brightness temperatures in excess of 10^8 K.

3. RATES OF MOTION

Careful inspection of the top three frames of Fig. 1 indicates apparent motion of the flare source to the north–east. To determine the rate of movement of the flare sources we rotated the images $\sim 50°$ west of north so that motion was approximately along the vertical axis, and then measured the centroids of discrete features in the LCP images (corresponding features are seen in the RCP images in virtually all cases) using two dimensional Gaussian fits. The results are plotted in Figure 2. The clearest example of motion is the initial change seen in the top 3 panels of Figure 1. These are the points joined by a solid line in Fig. 2. This line (through the points at 20:24:31 and 20:24:37) has a slope of 37″ per second. The corresponding velocity of the emission feature transverse to the line of sight is 26000 km s^{-1}. At 20:24:44 a feature is present in the RCP image (which has lower noise levels) at least 500″ from the original flare site, and this is also consistent with a velocity of 26000 km s^{-1}. This same location appears bright in later LCP images. Fig. 2 illustrates the sporadic nature of the brightenings also evident in Fig. 1: some locations emit continuously once the disturbance passes by, while others fade and then reappear. In the region between 250″ and 500″ from the original position the radio source is large and the plotted positions are those of the brightest peaks.

The soft and hard X–ray images during the period of the motion (Silva et al. 1996) show only emission in the location marked in the first panel of Fig. 1. The subsequent appearance of even more distant radio sources clearly suggests the presence of a moving disturbance which excites emission at specific locations as it passes by. Scattering and ducting are known to affect the apparent height of sources (Duncan 1978) as well as their size, but is not believed to produce the transverse shifts of hundreds of arcseconds in a specific direction seen here, and it would be difficult to explain why the flare source but not the noise storm emission is shifted. The initial apparent motion could be mimicked by the simultaneous fading of the source at the flare location and the brightening of an adjacent source 130″ to the north–east; we return to this point later in the discussion.

The velocities inferred for this event are highly supersonic. The high brightness temperature of the flare source and its *o* mode sense of polarization suggest that it is due to plasma emission at the fundamental (ambient density 1.3×10^9 cm^{-3}) or second harmonic (3.4×10^8 cm^{-3}) of the plasma frequency. With the magnetic field in the quiet solar corona outside the active region unlikely to exceed 10 G, the Alfvén speed $2 \times 10^{11}\, B/\sqrt{n_e}$ will be less than 500 km s^{-1} and magnetoacoustic Mach numbers in excess of 40 are implied.

4. DISCUSSION

The relationship of this radio emission to recognized radio burst types is not immediately clear. The emission is observed at 0.33 GHz, is weakly polarized in a sense consistent with plasma emission, shows very rapid motion in images, and extends over a large area. RSTN data at 0.245 GHz show a time profile similar to that of the VLA 0.33 GHz data but reaching a peak of 600 sfu, while at 0.41 GHz the emission is relatively weak, suggesting that the emission was a continuum at least 100 MHz wide. Classical shock–associated coronal Type II radio bursts (Nelson & Melrose 1985) are generally weakly polarized (less than 20%), show little motion at a given frequency (since emission is at the plasma frequency and the layer corresponding to a particular frequency, i.e., a particular density, is fixed), are only rarely seen above 0.3 GHz, usually have smaller bandwidths than we infer for this event, but their durations at a given frequency are similar. Moving Type IV bursts (Stewart 1985) are relatively broadband continua which show motion in images, are usually weakly polarized (at first) and are also usually confined to frequencies below 0.3 GHz. The duration of this event would also be shorter than any previously identified moving Type IV. No Type II or Type IV event was reported by radiospectrograph observations. We therefore cannot clearly identify this event with known burst types, but on the basis of the observed motion of the source at a fixed frequency it most closely resembles a moving Type IV burst. On the other hand, any disturbance travelling at 26000 km s^{-1} through the solar atmosphere must be supersonic and generate a strong shock.

The velocity inferred from our observation is large compared to velocities inferred for other coronal transients and shock speeds. The highest reported metric Type II speed is 13000 km s^{-1} (inferred from the frequency drift rate) in a GOES class X13 event (Nakajima et al. 1990). Gergely et al. (1983) reported a metric Type II burst which showed a plane-of-the-sky speed of 4900 km s^{-1} as it swept from 70 MHz down to 40 MHz. Moving Type IV bursts have been observed up to 1600 km s^{-1} (Robinson 1978; Kai 1979), while one Clark Lake event may have been as high as 2800 km s^{-1} (Gopalswamy & Kundu 1990). CME speeds can be as high as 2000 km s^{-1} (Hundhausen et al. 1994), and Moreton waves can be up to 4000 km s^{-1} (Sakurai et al. 1995).

A striking feature of Fig. 2 is the apparent abrupt shift in source location from $0''$ to $\sim 130''$ (in the units of the vertical axis) at the start of the event. By considering the relative locations of the 0.33 and 1.4 GHz sources we can suggest one scenario for this event. The lower left panel of Fig. 1 shows that two 1.4 GHz sources lie at either end of the elongated source which is closest to the original flare site. The two 1.4 GHz sources are both highly polarized and have high brightness temperatures, implying that they are due to a coherent emission mechanism. They have similar time profiles. However, the more northern of these two locations is known to be connected to the original flare site by a loop seen in soft X–rays (Silva et al. 1996). No such connection exists to the southern 1.4 GHz source. We speculate that the sudden shift in the 0.33 GHz source position is associated with the formation of a new magnetic connection between the central positive magnetic polarity region of AR 6994 (near the original flare location) and the trailing negative polarity region. The southern 1.4 GHz source may represent one footpoint of this loop system. Since the 0.33 GHz emission at the original flare location (at distance $0''$ in Fig. 2) fades when the new loop (at distance

130″) is established, field lines initially located in the original flare source may have "jumped" to the location of the new source, sending some form of disturbance in that direction (to the north–east) which continues to propagate beyond the active region. This disturbance does not itself radiate but somehow it excites discrete coronal features which continue to radiate after the disturbance has passed by. This scenario does not address the manner in which radio emission at more distant locations is excited by the disturbance.

5. CONCLUSIONS

Radio images of a flare at 0.33 GHz show source motions in the plane of the sky at ~ 26000 km s^{-1} or faster. The initial motion occurs in an elongated source located at the flare site which is stationary for some unknown period prior to the onset of motion. The subsequent motion is not the steady motion of a single isolated source, but a succession of brightenings at increasing distances from the flare site. The properties of the radio emission (weak circular polarization, bandwidth in excess of 100 MHz, rapid motion on the sky at a fixed frequency, high brightness temperature) imply plasma emission: the motion suggests a moving Type IV radio burst rather than a Type II radio burst. However, at this speed a shock must be associated with the disturbance. Motion is not omnidirectional, but rather in a specific direction (in this case, to the north–east across disk center). Before fading, the flare radio source attains a size of over 500″. The observed speed is the highest speed yet directly measured for a disturbance other than freely streaming energetic electrons. We speculate that the disturbance may be generated by a realignment of magnetic fields connecting different portions of an active region. The disturbance itself does not seem to radiate, but it excites coronal features which continue to radiate after it passes. The velocity is comparable to or larger than the highest velocities reported for Moreton waves, Type II shocks and moving Type IV bursts, and is well in excess of any speed so far detected by EUV or soft X–ray emitting material.

Acknowledgments

This research at the University of Maryland was carried out with support from NSF grant ATM 96-12738 and NASA grants NAG 5-7370, NAG 5-6257 and NAG 5-7901. We thank Alexander Nindos for valuable comments and advice, and Helen Coffey and Susan Wahl for providing RSTN data.

REFERENCES

Athay, R. G. & Moreton, G. E. 1961, ApJ, 133, 935

Bastian, T. 1994, ApJ, 426, 774

Duncan, R. A. 1978, Proc. Astron. Soc. Aust., 3, 253

Gergely, T. E., Kundu, M. R., & Hildner, E. 1983, ApJ, 268, 403

Gopalswamy, N. & Kundu, M. R. 1990, Solar Phys., 128, 377

Hundhausen, A. J., Burkepile, J. T., & St Cyr, O. C. 1994, J. Geophys. Res., 99, 6543

Kai, K. 1979, Solar Phys., 61, 187

Kai, K., Melrose, D. B., & Suzuki, S. 1985, in Solar Radiophysics, ed. D. J. McLean & N. R. Labrum (Cambridge: Cambridge University Press), 415

MacQueen, R. M., Eddy, J. A., Gosling, J. T., Hildner, E., Munro, R. H., Newkirk, Jr., G. A., Poland, A. I., & Ross, C. L. 1974, ApJL, 187, L85

Melrose, D. B. 1985, in Solar Radiophysics, ed. D. J. McLean & N. R. Labrum (Cambridge: Cambridge University Press), 289

Moreton, G. F. 1961, S&T, 21, 145

Nakajima, H., Kawashima, S., Shinohara, N., Shiomi, Y., Enome, S., & Rieger, E. 1990, ApJS, 73, 177

Nelson, G. J. & Melrose, D. B. 1985, in Solar Radiophysics, ed. D. J. McLean & N. R. Labrum (Cambridge: Cambridge University Press), 333

Ramsey, H. E. & Smith, S. F. 1966, AJ, 71, 197

Robinson, R. D. 1978, Solar Phys., 60, 383

Sakurai, T., Irie, M., Miyashita, K., Yamaguchi, K., & Shiomi, Y. 1995, in Proc. Second SOLTIP Symposium, ed. T. Watanabe (STEP (GBRSC News, Spec. Issue 5)), 33

Shibata, K., Ishido, Y., Acton, L. W., Strong, K. T., Hirayama, T., Uchida, Y., McAllister, A. H., Matsumoto, R., Tsuneta, S., Shimizu, T., Hara, H., Sakurai, T., Ichimoto, K., Nishino, Y., & Ogawara, Y. 1992, PASJ, 44, L173

Silva, A. V. L., White, S. M., Lin, R. P., de Pater, I., Gary, D. E., McTiernan, J. M., Hudson, H. S., Doyle, J. G., Hagyard, M. J., & Kundu, M. R. 1996, ApJS, 106, 621

Stewart, R. T. 1985, in Solar Radiophysics, ed. D. J. McLean & N. R. Labrum (Cambridge: Cambridge University Press), 361

Thompson, B. J., Gurman, J. B., Neupert, W. M., Newmark, J. S., Delaboudiniére, J., St Cyr, O. C., Stezelberger, S., Dere, K. P., Howard, R. A., & Michels, D. J. 1999, ApJL, 517, L151

Weiss, A. A. 1963, Aust. J. Phys., 16, 526

Wild, J. P. 1950a, Aust. J. Sci. Res., A3, 541

—. 1950b, Aust. J. Sci. Res., A3, 399

Wild, J. P., Murray, J. D., & Rowe, W. C. 1954, Aust. J. Phys., 7, 439

This preprint was prepared with the AAS LaTeX macros v5.0.

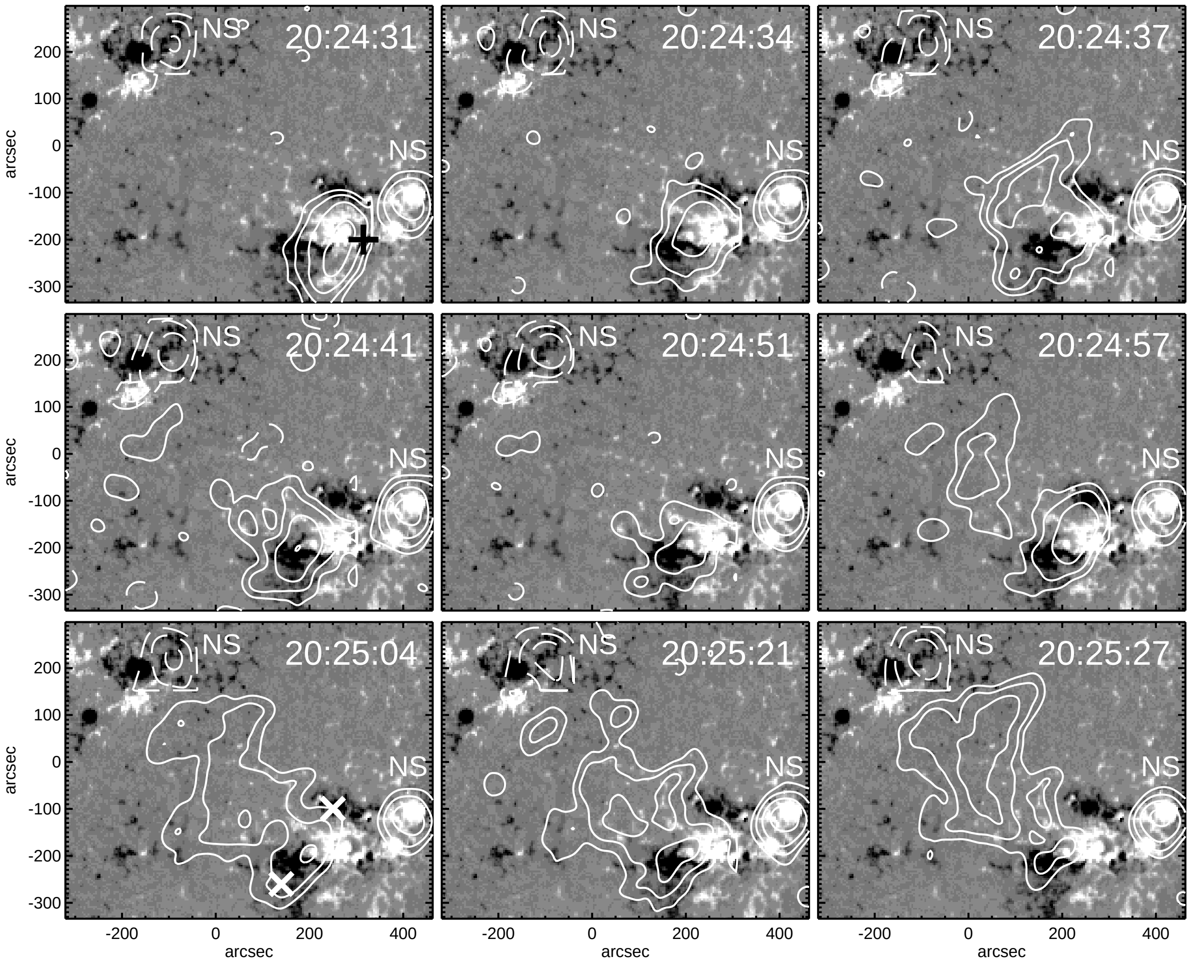

Fig. 1.— VLA images of the radio emission at 333 MHz at selected times (contours) overlaid on a Kitt Peak magnetogram. In order not to clutter the figures with too many lines, the contours represent a composite image. Solid contours show left circularly polarized (LCP) emission. For the strong compact non–flare noise storm source at the right edge of the panel (labelled "NS") which is 100% LCP, contours are plotted at 2, 4, 8 & 16 sfu per beam. For the compact noise storm source at the top left of the panels (also labelled "NS" and shown in dashed contours since it is 100% right circularly polarized), contours are plotted at 0.25, 0.5 & 1 sfu per beam. The flare emission and moving source are shown by contours in the region between these two compact noise storms, with contours at 0.5, 1, 2 & 4 sfu per beam. The average noise level in all the LCP maps is about 0.2 sfu/beam, set largely by the brightness of the LCP noise storm. In the corresponding RCP maps it is somewhat lower. The time of each image is shown in the upper right corner, and the axes of the panels are labelled in arcseconds east–west and north–south with the origin at apparent disk center. The location of the optical and X–ray flare emission is indicated by a plus symbol in the top left panel, while two white cross symbols in the bottom left panel show the location of emission at 1.4 GHz during the period discussed.

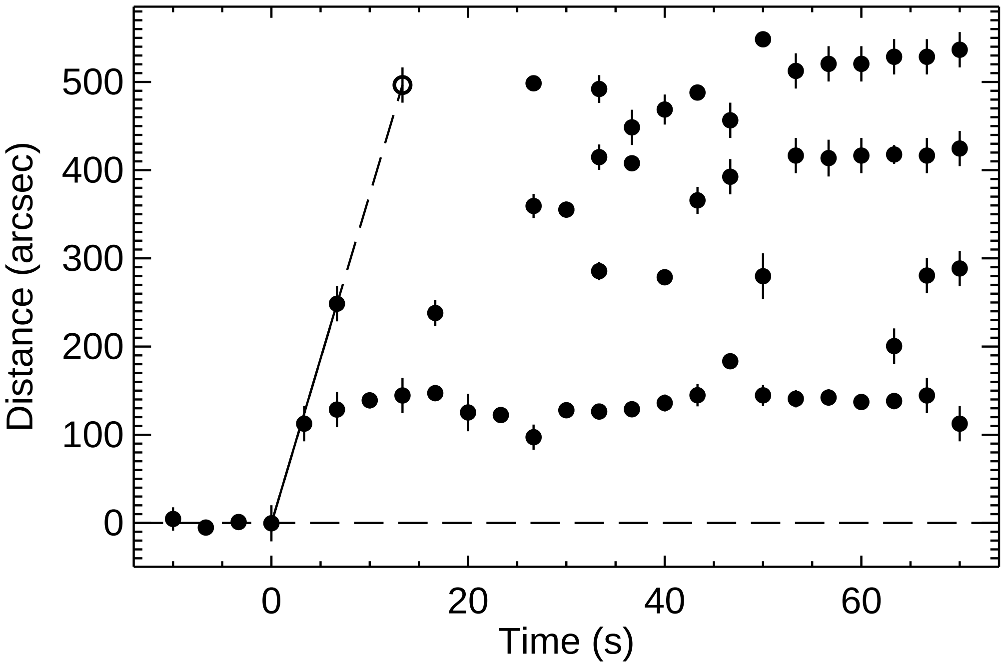

Fig. 2.— Locations of emission features at LCP (filled circles) as a function of time relative to the initial position of the flare source. The distance is measured in a direction corresponding to the inferred direction of motion, i.e., about 50° east of north, and positions shown are the positions of the centroids of discrete bright features in each 3.3 s snapshot image. At later times more than one emission feature may be present in each image. The zero on the time axis corresponds to 20:24:31 UT. Error bars represent approximately the size of the source in the direction of motion. The solid line shows the fit to the motion seen in the top 3 panels of Fig. 1. The open circle shows the position of a source seen in the RCP image (which has a lower noise level than the LCP images) at 20:24:44, and the dashed line joins it to the point at time zero.